ACS APPLIED MATERIALS & INTERFACES

Research Article

www.acsami.org

Novel Stable Gel Polymer Electrolyte: Toward a High Safety and Long Life Li–Air Battery

Jin Yi,[†] Xizheng Liu,[†] Shaohua Guo,[†] Kai Zhu,[†] Hailong Xue,[†] and Haoshen Zhou*[,†,‡]

[†]Energy Technology Research Institute, National Institute of Advanced Industrial Science and Technology (AIST), 1-1-1, Umezono, Tsukuba, 305-8568, Japan

[‡]National Laboratory of Solid State Microstructures and Center of Energy Storage Materials and Technology, Nanjing University, Nanjing, 210093, China

Supporting Information

ABSTRACT: Nonaqueous Li–air battery, as a promising electrochemical energy storage device, has attracted substantial interest, while the safety issues derived from the intrinsic instability of organic liquid electrolytes may become a possible bottleneck for the future application of Li–air battery. Herein, through elaborate design, a novel stable composite gel polymer electrolyte is first proposed and explored for Li–air battery. By use of the composite gel polymer electrolyte, the Li–air polymer batteries composed of a lithium foil anode and Super P cathode are assembled and operated in ambient air and their cycling performance is evaluated. The batteries exhibit enhanced cycling stability and safety, where 100 cycles are achieved in ambient air at room temperature. The feasibility study demonstrates that the gel polymer electrolyte-based polymer Li–air battery is highly advantageous and could be used as a useful alternative strategy for the development of Li–air battery upon further application.

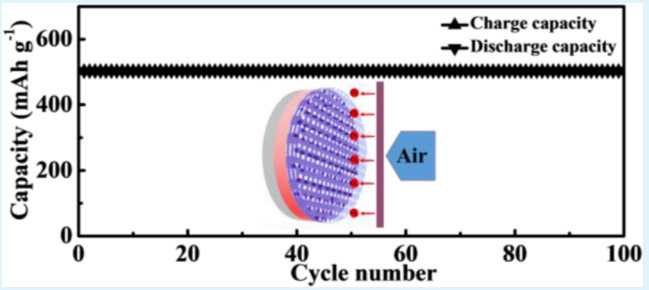

KEYWORDS: *stable, safety, gel polymer electrolyte, liquid-free, Li–air battery*

1. INTRODUCTION

The development of electric vehicles (EVs) and hybrid electrical vehicles (HEVs) is considered to be an attractive route to solve the energy crisis issues, and a large number of achievements have been obtained under worldwide efforts. However, the successful further application of EVs and HEVs depends to a great extent on the power and energy densities of batteries.[1−4] As a promising alternative to Li-ion battery, rechargeable Li–air battery with theoretical energy density of about 3500 Wh kg^{-1} deserves to receive much concern since the first rechargeable lithium/oxygen battery was reported in 1996 by Abraham.[5] Its implementation for energy storage in vehicle applications has been slowed by safety concerns due to the Li–air batteries with an open system using the volatile and flammable organic liquid electrolytes. Some undesired reactions could be triggered by unpredictable events such as short circuits or local overheating, producing a rapid increase of the battery temperature and, eventually, to fire or explosion and remaining a hurdle for market penetration of Li–air battery in the future practical large-scale application.[6−9] It is thereby of great urgency to develop novel safe electrolytes for Li–air battery, where replacing liquid electrolytes with polymer electrolytes would be a perfect solution to those safety issues.[10] Solid polymer electrolytes (SPEs) have been considered as ideal alternatives to liquid electrolytes, and many efforts have been made to develop SPE for Li–air battery with the aim to achieve a satisfying electrochemical performance.[11] However, their low ionic conductivity (10^{-8} to 10^{-5} S cm^{-1}) and high interfacial resistance preclude their practical applications in Li–air battery at ambient temperature.[6] Fortunately, the gel polymer electrolyte (GPE), a transition state between liquid electrolyte and SPE, seems to be a smart choice, which uses polymer as a matrix to encapsulate liquid components. It is this unique character that makes GPEs key materials for the development of high safety Li–air battery. Unlike a conventional Li–air battery with the cathode flooded with liquid electrolyte, the "three-phase reaction zone" would be formed in the Li–air battery using GPE due to the absence of the flooding electrolyte, as illustrated in Figure 1, which would be greatly beneficial to avoiding the blocked pores and enhancing the diffusion of oxygen in cathode, subsequently improving the performance of Li–air battery. Therefore, the development of high safety Li–air battery as power source of EVs and HEVs may greatly benefit from a switch to GPE. Moreover, the GPE is also more flexible and can provide additional benefits in scalability and processability compared with conventional inorganic glass or ceramic electrolytes, which enables them to assemble different shapes according to the practical requirements.[12,13] However, some limited success has been achieved to explore GPE for Li–air battery except for poly(vinylidene

Received: September 9, 2015
Accepted: October 9, 2015
Published: October 9, 2015

DOI: 10.1021/acsami.5b08462
ACS Appl. Mater. Interfaces 2015, 7, 23798−23804

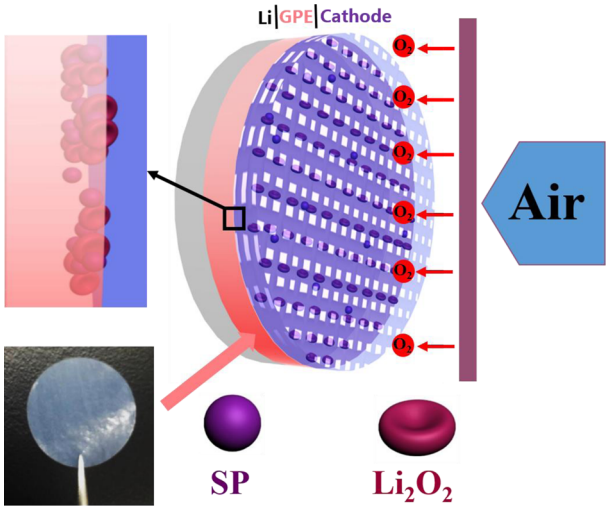

Figure 1. Schematic illustration of the proposed GPE-based polymer Li−air battery.

fluoride-*co*-hexafluoropropylene) (P(VdF-HFP))-based GPE[14−16] and natural rubber polymer.[17] Additionally, the host polymers would lose mechanical strength when plasticized by organic solvents, which can be overcome through a mechanical skeleton, such as polyethylene (PE), polypropylene (PP), and nonwoven fabrics.[18,19] Meanwhile, to obtain the GPEs with improved ionic conductivity and interfacial properties at the lithium electrode, ceramic fillers, such as TiO_2, SnO_2, MgO, Al_2O_3, and SiO_2 have been incorporated into host polymers.[20−24] Last but not least, owing to the existence of oxygenated radicals produced during the discharge process, some polymer compounds will be oxidized and unstable in the presence of Li_2O_2, such as P(VdF-HFP), poly(ethylene oxide) (PEO), polyacrylomtrile (PAN), poly-(vinyl chloride) (PVC), poly(vinylidene fluoride) (PVDF), and poly(vinylpyrrolidone) (PVP).[25−27] Thus, comprehensive work is required to address the stability issue of polymer-based electrolytes, and the exploration of stable GPE becomes significant for achieving Li−air battery with long operating life.

On the basis of the above background, in this study, a novel stable GPE, polypropylene (PP)-supported poly(methyl methacrylate) (PMMA)−blend−poly(styrene) (PSt) with doping nanofumed SiO_2, hereafter referred to as PMMA/PSt/SiO_2/PP, has been subtly designed and explored for Li−air battery. The implementation of blended polymers here is proposed with the aim of balancing the advantanges and drawbacks of components. By use of the GPE, a Li−air polymer battery composed of a lithium foil anode and a SP cathode without any other catalysts is proposed. The cycling performance of the batteries was evaluated and compared with that of the batteries assembled with liquid electrolyte. Our results demonstrate the superior performance of Li−air polymer batteries using a PMMA/PSt/SiO_2/PP-based composite polymer electrolyte and report a new step toward the realization of commercial Li−air battery.

2. EXPERIMENTAL SECTION

2.1. Chemical Stability Test of PSt. The chemical stability test of PSt was performed in a argon-filled glovebox (H_2O < 0.1 ppm, O_2 < 0.1 ppm). The following describes a typical experiment. In a 15 mL vial, 20 mg of PSt was dissolved in 5 mL of tetrahydrofuran (THF) (stored in the presence of a shining Li foil). The polymer/solvent mixture was stirred to allow the polymer to dissolve. Then 200 mg of Li_2O_2 was added to allow for an excess mass concentration of Li_2O_2 as compared to the polymer mass concentration. The mixture was stirred throughout the course of the experiment.

2.2. Preparation of Gel Polymer Electrolytes. The obtained polymer (PMMA, PSt), 2.4 wt % polyethylene glycol (PEG, molecular weight 400, as a pore producer) and 10 wt % nanofumed SiO_2 (Sigma-Aldrich, average particle size of 7 nm) with content of polymer were dispersed in THF at a concentration of 4 wt % under stirring. After complete dissolution, a commercial microporous polypropylene (PP) separator (Celgard, USA, thickness of 25 um) was immersed in the slurry for 1 h, taken out, and transferred into a sink for phase inversion. The resulting membrane was washed with deionized water and immersed into deionized water for 2 h to remove residual PEG and THF. The porous PMMA/PSt/SiO_2/PP membrane was finally obtained after drying the membrane in vacuum at 50 °C for 24 h. In order to prepare GPE, the porous membranes were immersed in an electrolyte solution, 1 M bis(trifluoromethane) sulfonimide lithium salt (LiTFSI, Sigma-Aldrich, 99.95%) in tetraethylene glycol dimethyl ether (TEGDME, G4, Sigma-Aldrich, 99%), in an argon-filled glovebox with water and oxygen content lower than 0.1 ppm overnight before use. For comparison, the 1 M LiTFSI/G4 and commercial PP were used as conventional liquid electrolyte and separator, respectively.

2.3. Characterization. X-ray powder diffraction (XRD) patterns were recorded on a Bruker D8 X-ray diffractometer using Cu Kα (λ = 1.54 Å) radiation. The images of all the samples and electrodes were examined using scanning electronic microscope (SEM) on a JSM-6700F instrument. The discharged and recharged SEM cathodes were washed with diethyl carbonate (DEC) followed by removal of the DEC in vacuum. The thermogravimetric analysises (TGA) were conducted on BRUKER TG-DTA 2010SA-G4H to survey thermal stability of the PMMA/PSt/SiO_2/PP membrane.

2.4. Electrochemical Characterization. The electrochemical stability of GPE was investigated by the linear sweep voltammograms, which was obtained on Solartron 1640 at a scanning rate of 1.0 mV s^{-1}, where GPE was sandwiched between lithium anode and SS. The compatibility of GPE with the anode of Li−O_2 battery was understood by electrochemical impedance spectroscopy (EIS) using the symmetrical cell Li/GPE/Li with potential amplitude of 5 mV from 0.1 to 100 kHz. The ionic conductivity of the GPE was determined by the symmetrical cell SS/GPE/SS using EIS with potential amplitude of 5 mV from 0.1 to 100 kHz. All of the above electrochemical measurements were conducted at 25 °C and in 1 atm of O_2 flow. The Super P (SP) cathode was prepared by first mixing SP, PTFE together with a weight ratio of 85:15 and rolled into a film, which was pressed onto carbon based gas diffusion layer (GDL 35BA, SIGRACET Gas Diddusion Media) as cathodes. The electrodes were dried at 100 °C in a vacuum oven for 12 h. The total mass loading of SP is about 1 mg cm^{-2}. The cells were assembled in an argon filled glovebox with water and oxygen level less than 0.1 ppm. A lithium foil was used as anode. The as-prepared GPE was sandwiched between a lithium anode and a SP cathode. The cells were gastight except for the cathode side window, which exposed the cathode film to the oxygen and air atmosphere. For the tests in dry oxygen atmosphere, the measurements were conducted in 1 atm of dry oxygen to avoid any negative effects of humidity and CO_2. For the tests in ambient air, the as-obtained cells were kept in a glass chamber filled with argon gas and then taken out from the glovebox. Pure O_2 flowed through the glass chamber to replace the argon gas. After that, the ambient air was allowed to permeate by opening the cover, and then the RH was adjusted to 5 by continuing to flow the dry air (mixture of N_2/O_2 (22.1%)) through the glass chamber. Galvanostatic discharge/charge tests were conducted on the Hokuto discharge/charge system at 25 °C within the potential window between 2 and 4.8 V under different capacity limit.

DOI: 10.1021/acsami.5b08462
ACS Appl. Mater. Interfaces 2015, 7, 23798−23804

3. RESULTS AND DISCUSSION

In order to investigate the chemical stability of PSt in the presence of Li_2O_2, the PSt was stirred with commercial Li_2O_2 for 30 days. From the results shown in Figure S1 in Supporting Information, it can be seen that PSt appears stable against nucleophilic attack of Li_2O_2 without obvious color change, compared with the obvious color change for the PAN, PVDF, and P(VdF-HFP) in the reported results.[16] The lack of labile hydrogen atoms and the poor leaving nature of the phenyl group are responsible for the stability of PSt against nucleophilic attack of Li_2O_2. Figure 2a presents the X-ray

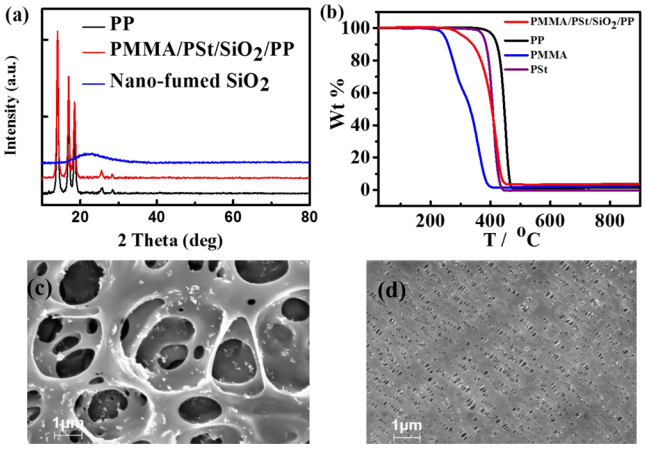

Figure 2. (a) XRD patterns of PP, PMMA/PSt/SiO_2/PP membrane, nanofumed SiO_2. (b) TG profiles of PMMA/PSt/SiO_2/PP based membrane, PP, PMMA, and PSt. SEM images of PMMA/PSt/SiO_2/PP membrane (c) and PP (d).

diffraction (XRD) patterns of PP, PMMA/PSt/SiO_2/PP, and nanofumed SiO_2. The integrated XRD intensity exhibits the typical α-form PP crystals and complete absence of the β-crystal form, which shows two strong peaks at 2θ of 16.2° and 21.2°.[28,29] Meanwhile, the PMMA/PSt/SiO_2/PP displays a similar XRD pattern to the PP, indicating that the blended polymer and nanofumed SiO_2 exist in the amorphous form, and amorphous structure favors the chain movement of the polymer during the membrane formation and leads to the formation of more interconnected pores in the membrane. The thermal stability of PMMA/PSt/SiO_2/PP and PP membranes, PMMA, PSt was determined by TGA under Ar atmosphere from room temperature to 900 °C at a heating rate of 10 °C min^{-1}, and the results are provided in Figure 2b. It can be seen that the thermal stability of PMMA/PSt/SiO_2/PP membrane has been deteriorated after blending the PMMA, compared with PP membrane. However, in these cases, the limitation arising from the thermal stability of the used polymer is negligible because the decomposition temperature is higher than the shutdown temperature.[30,31] Figure 2c and Figure 2d display SEM images of PMMA/PSt/SiO_2/PP membrane and PP. In the phase inversion process, the porous structure is formed by the exchange between solvent (THF) and nonsolvent (water). It can be seen from Figure 2c that after doping fumed silica and upon the introduction of PEG, porous structure (on and under the surface of the membrane) can be seen clearly, resulting in the improved porosity (P) (45%) and electrolyte uptake (A) (212%), which are evaluated based on the following eqs 1 and 2.

$$P = \frac{\frac{m_a}{\rho_a}}{\frac{m_a}{\rho_a} + \frac{m_p}{\rho_p}} \quad (1)$$

where ρ_a and ρ_p are the density of n-butanol and the dry membrane, respectively. m_a and m_p are the mass of the membrane after n-butanol incorporated for 2 h and the dry membrane, respectively.

$$A\ (\%) = \frac{W_2 - W_1}{W_1} \times 100 \quad (2)$$

where W_1 and W_2 are the mass of the dry and wet membranes, respectively, where the wet membrane was obtained by immersing the membrane in the same solution as that for GPE preparation for 0.5 h.

Besides, it can be found that the as-prepared PMMA/PSt/SiO_2/PP membrane has good affinity to the 1 M bis-(trifluoromethane) sulfonimide lithium salt (LiTFSI)/tetraethylene glycol dimethyl ether (TEGDME, G4) electrolyte, and the as-obtained GPE appears almost transparent, while the PP shows bad affinity to the electrolyte (Figure S2), and the good affinity will be beneficial to avoiding the blocked pores by flooding liquid electrolyte and enhancing the diffusion of oxygen in cathode, further achieving improved electrochemical performance.

Tolerance to high potential is very important for GPE, especially for the development of long life Li−air batteries. To obtain further insight concerning the electrochemical stability of the as-prepared GPE, the linear sweep voltammograms were carried out at a scanning rate of 1 mV s^{-1}. Figure 3a gives linear

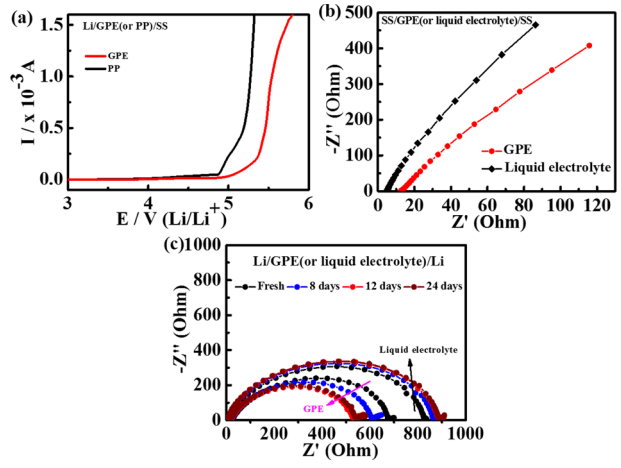

Figure 3. (a) Linear sweep voltammograms for PMMA/PSt/SiO_2/PP based GPE and PP (liquid electrolyte), with scanning rate of 1 mV s^{-1}. (b) Nyquist plots of GPE and liquid electrolyte with the cell structure of stainless steel (SS)/GPE (or liquid electrolyte)/SS. (c) Evolution of the impedance spectra of Li/GPE (or liquid electrolyte)/Li cell at open circuit potential as a function of time. All of the tests were carried out in O_2 environment.

sweep voltammograms obtained for the battery Li/GPE/SS, compared with the battery Li/liquid electrolyte/SS. It can be seen that the liquid electrolyte decomposes from about 4.8 V (vs Li/Li^+), while the decomposition potential of GPE has been increased to 5.3 V (vs Li/Li^+), indicative of the improvement in oxidative stability of the as-prepared GPE. This improvement can be ascribed to the improved stability of electrolyte components that are trapped more tightly in the membrane

DOI: 10.1021/acsami.5b08462
ACS Appl. Mater. Interfaces 2015, 7, 23798−23804

with fumed silica. Sufficient conductivity is one of the key factors for maintaining a smooth transport of lithium ions in GPEs for Li−air batteries. The ionic conductivity of the as-prepared GPE is calculated according to the bulk electrolyte resistance (R_b), where they are obtained from the intercept of the straight line on the real axises (as shown in Figure 3b). On the basis of eq 3, the obtained ionic conductivities are 1.27 × 10^{-4} S cm^{-1} for GPE and 2.48 × 10^{-4} S cm^{-1} for liquid electrolyte, indicating that as-prepared GPE has attractive ionic conductivity for the application in Li−O_2 battery and lithium ion battery (Figure S3).[16,32]

$$\sigma = \frac{d}{R_b S} \tag{3}$$

where d is the thickness of GPE, and S is the contact area between GPE and SS disk (diameter Φ = 16 mm).

Through elaborate design, the PMMA/PSt/SiO_2/PP-based GPE thus provides more routes for the ionic transportation, resulting in the enhancement of ionic conductivity. Interfacial stability of GPE with lithium metal anode of Li−O_2 battery is another essential factor to guarantee high performance of the Li−O_2 batteries, which is associated with the passive layer and the charge transfer resistances on the lithium electrode. In order to get the interfacial resistance between GPE and lithium metal anode, electrochemical impedance spectroscopy of the cells Li/GPE/Li at open circuit was monitored with time as described in Figure 3c, where the semicircle at high frequencies reflects the resistance of passive film on lithium. It can be seen from Figure 3c that the resistance of the passive film of GPE is smaller than PP, which means that the as-prepared GPE has much better compatibility with lithium metal anode than liquid electrolyte. Moreover, the resistance of the passive film increases within 2 weeks, resulting from the continuous growth of a resistive layer on the lithium metal surface and remains almost unchanged after 2 weeks for liquid electrolyte, while the resistance of the passive film of GPE decreases within 2 weeks and remains almost unchanged after 2 weeks. From the above results, it can be concluded that the as-prepared GPE shows good compatibility with Li metal anode of Li−O_2 battery.

In order to get information on the electrochemical performance of Li−O_2 (air) batteries assembled with the as-prepared GPE, the systematic galvanostatic discharge/charge tests were performed under different conditions. It should be noted that the cathodes were fabricated by commercial SP and stable poly(tetrafluoroethylene) (PTFE) binder without any other catalysts.[26] Figure 4 provides the rate capability of Li−O_2 batteries assembled with GPE and liquid electrolyte with a fixed discharge capacity of 1000 mAh g^{-1} under different current densities. It can be seen that the PMMA/PSt/SiO_2/PP-based GPE exhibits a comparable rate capability with the liquid electrolyte. Therefore, the safety of Li−O_2 battery can be improved without sacrificing the electrochemical performance. Additionally, during the charge process, three voltage plateaus are displayed. At low potentials (at about 3.6 V) this may involve the decay of amorphous Li_2O_2, whereas at higher potentials (at 4.0−4.2 V), crystalline Li_2O_2 is decomposed via a Li deficient solid solution reaction, and the decomposition reaction of Li_2CO_3-like species may occur at 4.2−4.5 V.[33−35] The obvious difference from cycling stability of the cells using GPE and liquid electrolyte at the current density of 200 mA g^{-1} is displayed in Figure 5a and Figure 5b, in which more than 50

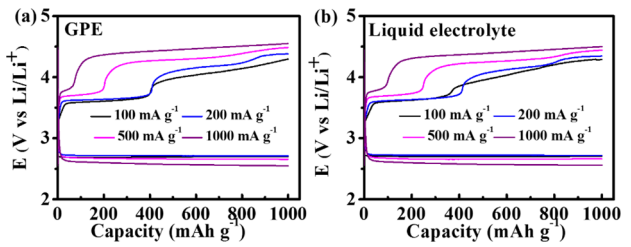

Figure 4. Rate capability of Li−O_2 batteries assembled with (a) as-prepared GPE and (b) liquid electrolyte under different current densities under dry O_2.

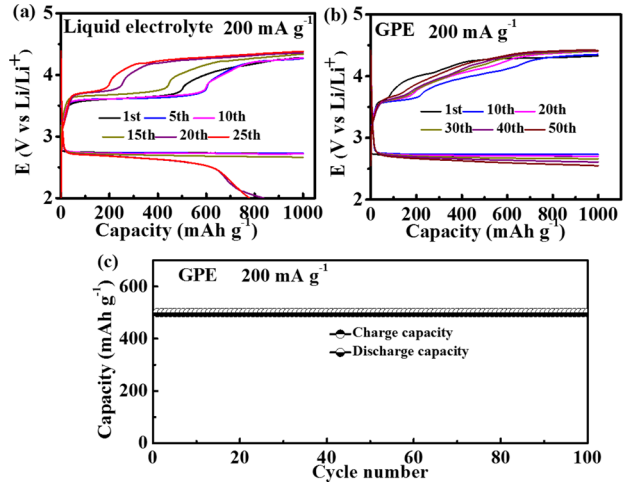

Figure 5. Discharge/charge curves of the Li−O_2 batteries using (a) liquid electrolyte, (b) as-prepared GPE with a capacity limit of 1000 mAh g^{-1}, and (c) cyclic performance the Li−O_2 battery assembled with GPE at a fixed capacity of 500 mAh g^{-1}. All of the cycling tests were operated at a current density of 200 mA g^{-1} under dry O_2.

cycles are achieved using GPE, while only 15 cycles are achieved by using liquid electrolyte. Therefore, in contrast with conventional liquid electrolyte, significantly enhanced cycling stability is achieved in combination with the use of GPE, which is predominantly derived from the absence of flooded air electrodes and the increase of oxygen diffusion, together with the suppression of the dendrite formation during cycling.[36] Meanwhile, it cannot be negligible that the Li−O_2 batteries assembled with GPE still suffer from limited cyclability, mainly due to the formation of Li_2CO_3-like species or other reaction byproducts on the cathode surface during discharge and charge processes, resulting in high overpotential upon charging and eventually battery failure, according to the previous reported results. In order to decrease the effects of detrimental side reactions on the cyclic stability, the discharge capacity was controlled to 500 mAh g^{-1} (Figure 5c), and the cyclic performance for Li−O_2 battery assembled with GPE has been increased to 100 cycles (the corresponding discharge/charge profiles shown in Figure S4).

To obtain further insight concerning the morphology of discharge products and the reversibility of the formation and decomposition of Li_2O_2 under dry O_2, SEM and XRD experiments were conducted on the discharged and recharged cathodes. Compared with the pristine SP cathode given in Figure 6a, discharge product of Li_2O_2 with a toroids-like morphology appears in the SEM images collected after discharge (Figure 6b), similar to the previous results, and

DOI: 10.1021/acsami.5b08462
ACS Appl. Mater. Interfaces 2015, 7, 23798−23804

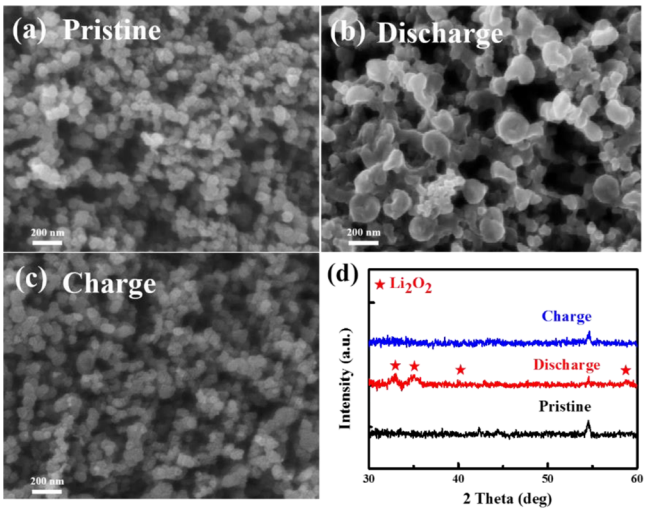

Figure 6. Morphologies of cathode at different states when using GPE as electrolyte under dry O_2: (a) pristine electrode, (b) after discharge, (c) after recharge, and (d) the corresponding XRD.

then they are removed during the recharging process (Figure 6c).[37−39] The reversible formation and decomposition of Li_2O_2 products are further supported by the XRD observations (Figure 6d). The diffraction peaks of Li_2O_2 can be clearly observed after discharge, which suggests that Li_2O_2 is the dominant crystalline product in the discharging process of the Li−O_2 battery with a SP cathode and GPE. Moreover, the above diffraction peaks of Li_2O_2 disappear after recharge, which means the reversible discharge and charge capacities mainly result from the desirable formation and decomposition of Li_2O_2.

Further research has been carried out to investigate the electrochemical performance of Li−air batteries assembled with GPE and liquid electrolyte operated in ambient air with relative humidity (RH) of 5. From Figure 7, it can be found that about 25 cycles are achieved when using GPE, which is more stable than liquid electrolyte in ambient air (8 cycles) and dry oxygen

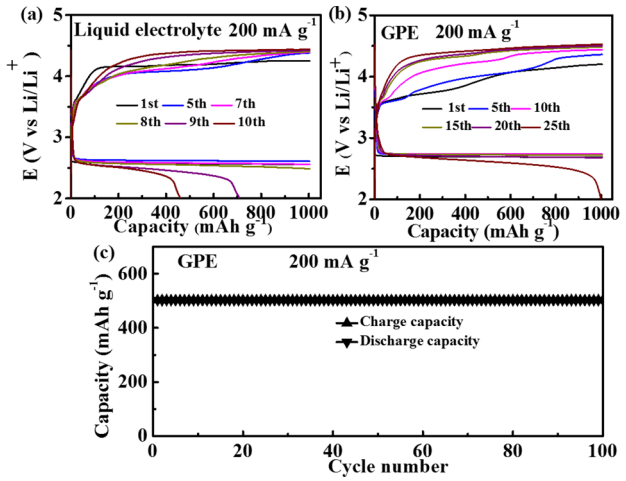

Figure 7. Discharge/charge profiles of the Li−air batteries assembled with (a) liquid electrolyte, (b) as-prepared GPE with a capacity limit of 1000 mAh g^{-1}, and (c) cyclic performance of the Li−air battery using GPE at a fixed capacity of 500 mAh g^{-1}. All of the cycling tests were operated at a current density of 200 mA g^{-1} under ambient air with RH of 5.

(15 cycles). The improvement in cyclic life is attributed to the swelled polyether (TEGDME) in the GPE which alleviates the corrosion of lithium metal caused by the H_2O contamination and subsequently facilitates improvement of the anode stability during cycling. Moreover, when fixing the discharge capacity to 500 mAh g^{-1}, more than 100 cycles have been achieved even in ambient air with RH of 5 by using GPE (the corresponding discharge/charge profiles shown in Figure S5). The pronounced difference of cyclic stability in different discharge depth provides key evidence that the unsatisfying cyclic stability arises predominantly from the detrimental side reactions between Li_2O_2 and carbon. Therefore, further improvement of cycling stability can be achieved by the selection of a carbon-free cathode in future work to avoid these side reactions. These findings suggest that the as-prepared GPE can be significantly beneficial to improving the cycling performance of Li−air battery. From the above results and discussion, it can be concluded that a Li−air battery with significantly improved performance has been achieved in combination with the as-prepared GPE. One has to be aware, however, that the results presented here are preliminary and have to be improved through optimization of the components of GPE, while this discovery still provides a new avenue for the development of rechargeable Li−air battery with high safety and long life in future practical application. Additionally, experience and results gained from this work give critical suggestions in the bottom-up design of GPE for the future Li−air battery.

4. CONCLUSIONS

In summary, the results presented here illustrate the benefits of using GPE as electrolyte for liquid-free Li−O_2 battery with enhanced cyclic stability, which is predominantly beneficial from the absence of the blocked pores caused by the flooding liquid electrolyte and enhancement of the oxygen diffusion in cathode, together with the suppression of dendrite formation during cycling. Furthermore, the inhibition of Li metal corrosion has been achieved through alleviation of H_2O contamination. Therefore, the Li−air battery using the GPE can be cycled for 100 cycles even in ambient air, revealing a preliminary opportunity to move Li−O_2 to Li−air batteries with high safety by utilizing GPE. It is also worthwhile noting that this type of battery can be easily scaled up without concern of the safety issues caused by the leakage and/or uneven distribution of electrolytes. These achievements have motivated us to develop more performance-improved GPE for Li−air battery. This work also highlights the importance of GPE consideration in the development of Li−air batteries with alternative electrocatalysts (metal oxides, nonprecious and precious metals) and suggests realistic strategies for Li−air battery in future practical applications. However, the development of GPE-based Li−air batteries is still in its preliminary stage and subsequent work is needed to ensure their full exploitation. The challenge is in the choice of GPE that features high ionic conductivity combined with long operation life, as well as in the design of cathodes capable of ensuring excellent cyclic stability.

■ ASSOCIATED CONTENT

Supporting Information

The Supporting Information is available free of charge on the ACS Publications website at DOI: 10.1021/acsami.5b08462.

DOI: 10.1021/acsami.5b08462
ACS Appl. Mater. Interfaces 2015, 7, 23798−23804

Chemical stability of PSt in the presence of Li_2O_2, the affinity of PP for liquid electrolyte, electrochemical performance of $Li_4T_5O_{12}$ using the as-prepared GPE, discharge/charge curves of the Li–O_2 (air) battery using GPE at a fixed capacity of 500 mAh g^{-1} and a current density of 200 mA g^{-1} under dry O_2 and ambient air with RH 5 (PDF)

AUTHOR INFORMATION

Corresponding Author

*E-mail: hs.zhou@aist.go.jp.

Notes

The authors declare no competing financial interest.

ACKNOWLEDGMENTS

We are grateful for the partial financial support from the ALCA Project of JST, Japan.

REFERENCES

(1) Zhang, T.; Zhou, H. S. A Reversible Long-life Lithium–air battery in Ambient Air. *Nat. Commun.* **2013**, *4*, 1817.

(2) Zhang, K.; Zhang, L.; Chen, X.; He, X.; Wang, X.; Dong, S.; Han, P.; Zhang, C.; Wang, S.; Gu, L.; Cui, G. Mesoporous Cobalt Molybdenum Nitride: A Highly Active Bifunctional Electrocatalyst and Its Application in Lithium-O_2 Batteries. *J. Phys. Chem. C* **2013**, *117*, 858–865.

(3) Luo, W. B.; Chou, S. L.; Wang, J. Z.; Kang, Y. M.; Zhai, Y. C.; Liu, H. K. A Hybrid Gel-solid-state Polymer Electrolyte for Long-life Lithium Oxygen Batteries. *Chem. Commun.* **2015**, *51*, 8269–8272.

(4) Zhang, J. J.; Yue, L. P.; Hu, P.; Liu, Z. H.; Qin, B. S.; Zhang, B.; Wang, Q. F.; Ding, G. L.; Zhang, C. J.; Zhou, X. H.; Yao, J. H.; Cui, G. L.; Chen, L. Q. Taichi-inspired Rigid-flexible Coupling Cellulose-supported Solid Polymer Electrolyte for High-performance Lithium batteries. *Sci. Rep.* **2014**, *4*, 6272.

(5) Abraham, K. M.; Jiang, Z. A Polymer Electrolyte-Based Rechargeable Lithium/Oxygen Battery. *J. Electrochem. Soc.* **1996**, *143*, 1–5.

(6) Xu, K. Electrolytes and Interphases in Li-Ion Batteries and Beyond. *Chem. Rev.* **2014**, *114*, 11503–11618.

(7) Balaish, M.; Peled, E.; Golodnitsky, D.; Ein-Eli, Y. Liquid-Free Lithium–Oxygen Batteries. *Angew. Chem., Int. Ed.* **2015**, *54*, 436–440.

(8) Chang, Y. Q.; Dong, S. M.; Ju, Y. H.; Xiao, D. D.; Zhou, X. H.; Zhang, L. X.; Chen, X.; Shang, C. Q.; Gu, L.; Peng, Z. Q.; Cui, G. L. A Carbon- and Binder-Free Nanostructured Cathode for High-Performance Nonaqueous Li-O_2 Battery. *Adv. Sci.*, **2015**, *2*, DOI: 10.1002/advs.201500092.

(9) Lee, Y. S.; Lee, J. H.; Choi, J. A.; Yoon, W. Y.; Kim, D. W. Cycling Characteristics of Lithium Powder Polymer Batteries Assembled with Composite Gel Polymer Electrolytes and Lithium Powder Anode. *Adv. Funct. Mater.* **2013**, *23*, 1019–1027.

(10) Bonnet-Mercier, N.; Wong, R. A.; Thomas, M. L.; Dutta, A.; Yamanaka, K.; Yogi, C.; Ohta, T.; Byon, H. R. A Structured Three-dimensional Polymer Electrolyte with Enlarged Active Reaction Zone for Li-O_2 Batteries. *Sci. Rep.* **2014**, *4*, 7127.

(11) Hassoun, J.; Croce, F.; Armand, M.; Scrosati, B. Investigation of the O_2 Electrochemistry in a Polymer Electrolyte Solid-State Cell. *Angew. Chem., Int. Ed.* **2011**, *50*, 2999–3002.

(12) Liao, Y. H.; Rao, M. M.; Li, W. S.; Yang, L. T.; Zhu, B. K.; Xu, R.; Fu, C. H. Fumed Silica-doped Poly(butyl methacrylate-styrene)-based Gel Polymer Electrolyte for Lithium Ion Battery. *J. Membr. Sci.* **2010**, *352*, 95–99.

(13) Zhang, P.; Zhang, H. P.; Li, G. C.; Li, Z. H.; Wu, Y. P. A Novel Process to Prepare Porous Membranes Comprising SnO_2 Nanoparticles and P(MMA-AN) as Polymer Electrolyte. *Electrochem. Commun.* **2008**, *10*, 1052–1055.

(14) Zhang, D.; Li, R. S.; Huang, T.; Yu, A. S. Novel Composite Polymer Electrolyte for Lithium Air Batteries. *J. Power Sources* **2010**, *195*, 1202–1206.

(15) Jung, K. N.; Lee, J. I.; Jung, J. H.; Shin, K. H.; Lee, J. W.A Quasi-solid-state Rechargeable Lithium-oxygen Battery Based on a Gel Polymer Electrolyte with an Ionic Liquid. *Chem. Commun.* **2014**, *50*, 5458–5461.

(16) Zhang, J.; Sun, B.; Xie, X.; Kretschmer, K.; Wang, G. X. Enhancement of Stability for Lithium Oxygen Batteries by Employing Electrolytes Gelled by Poly(vinylidene fluoride-co-hexafluoropropylene) and Tetraethylene Glycol Dimethyl Ether. *Electrochim. Acta* **2015**, DOI: 10.1016/j.electacta.2015.03.103.

(17) Mohamed, S. N.; Johari, N. A.; Ali, A. M. M.; Harun, M. K.; Yahya, M. Z. A. Electrochemical Studies on Epoxidised Natural Rubber-based Gel Polymer Electrolytes for Lithium-air Cells. *J. Power Sources* **2008**, *183*, 351–354.

(18) Rao, M. M.; Liu, J. S.; Li, W. S.; Liang, Y.; Zhou, D. Y. Preparation and Performance Analysis of PE-supported P(AN-co-MMA) Gel Polymer Electrolyte for Lithium Ion Battery Application. *J. Membr. Sci.* **2008**, *322*, 314–319.

(19) Song, M. K.; Kim, Y. T.; Cho, J. Y.; Cho, B. W.; Popov, B. N.; Rhee, H. W. Composite Polymer Electrolytes Reinforced by Non-woven Fabrics. *J. Power Sources* **2004**, *125*, 10–16.

(20) Li, Z. H.; Zhang, H. P.; Zhang, P.; Li, G. C.; Wu, Y. P.; Zhou, X. D. Effects of the Porous Structure on Conductivity of Nanocomposite Polymer Electrolyte for Lithium Ion Batteries. *J. Membr. Sci.* **2008**, *322*, 416–422.

(21) Rao, M. M.; Liu, J. S.; Li, W. S.; Liao, Y. H.; Liang, Y.; Zhao, L. Z. Polyethylene-supported Poly(acrylonitrile-co-methyl methacrylate)/nano-Al_2O_3 Microporous Composite Polymer Electrolyte for Lithium Ion Battery. *J. Solid State Electrochem.* **2010**, *14*, 255–261.

(22) Xi, J. Y.; Qiu, X. P.; Cui, M. Z.; Tang, X. Z.; Zhu, W. T.; Chen, L. Q. Enhanced Electrochemical Properties of PEO-based Composite Polymer Electrolyte with Shape-Selective Molecular sieves. *J. Power Sources* **2006**, *156*, 581–588.

(23) Kim, J. K.; Cheruvally, G.; Li, X.; Ahn, J. H.; Kim, K. W.; Ahn, H. J. Preparation and Electrochemical Characterization of Electrospun, Microporous Membrane-based Composite Polymer Electrolytes for Lithium Batteries. *J. Power Sources* **2008**, *178*, 815–802.

(24) Liao, Y. H.; Rao, M. M.; Li, W. S.; Tan, C. L.; Yi, J.; Chen, L. Improvement in Ionic Conductivity of Self-supported P(MMA-AN-VAc) Gel Electrolyte by Fumed Silica for Lithium Ion Batteries. *Electrochim. Acta* **2009**, *54*, 6396–6402.

(25) Amanchukwu, C. V.; Harding, J. R.; Shao-Horn, Y.; Hammond, P. T. Understanding the Chemical Stability of Polymers for Lithium-Air Batteries. *Chem. Mater.* **2015**, *27*, 550–561.

(26) Harding, J. R.; Amanchukwu, C. V.; Hammond, P. T.; Shao-Horn, Y. Instability of Poly(ethylene oxide) upon Oxidation in Lithium–Air Batteries. *J. Phys. Chem. C* **2015**, *119*, 6947–6955.

(27) Nasybulin, E.; Xu, W.; Engelhard, M. H.; Nie, Z.; Li, X. S.; Zhang, J. G. Stability of Polymer Binders in Li-O_2 Batteries. *J. Power Sources* **2013**, *243*, 899–907.

(28) Shangguan, Y.; Song, Y.; Peng, M.; Li, B.; Zheng, Q. Formation of β-crystal from Nonisothermal Crystallization of Compression-molded Isotactic Polypropylene Melt. *Eur. Polym. J.* **2005**, *41*, 1766–1771.

(29) Seo, M. K.; Lee, J. R.; Park, S. J. Crystallization Kinetics and Interfacial Behaviors of Polypropylene Composites Reinforced with Multi-walled Carbon Nanotubes. *Mater. Sci. Eng., A* **2005**, *404*, 79–84.

(30) Wu, M. S.; Chiang, P. C. J.; Lin, J. C.; Jan, Y. S. Correlation between Electrochemical Characteristics and Thermal Stability of Advanced Lithium-ion Batteries in Abuse Tests-short-circuit Tests. *Electrochim. Acta* **2004**, *49*, 1803–1812.

(31) Venugopal, G.; Moore, J.; Howard, J.; Pendalwar, S. Characterization of Microporous Separators for Lithium-ion Batteries. *J. Power Sources* **1999**, *77*, 34–41.

(32) Kido, R.; Ueno, K.; Iwata, K.; Kitazawa, Y.; Imaizumi, S.; Mandai, T.; Dokko, K.; Watanabe, M. Li^+ Ion Transport in Polymer

DOI: 10.1021/acsami.5b08462
ACS Appl. Mater. Interfaces 2015, 7, 23798–23804

Electrolytes Based on a Glyme-Li Salt Solvate Ionic Liquid. *Electrochim. Acta* **2015**, *175*, 5.
(33) Ganapathy, S.; Adams, B. D.; Stenou, G.; Anastasaki, M. S.; Goubitz, K.; Miao, X. F.; Nazar, L. F.; Wagemaker, M. Nature of Li_2O_2 Oxidation in a Li-O_2 Battery Revealed by Operando X-ray Diffraction. *J. Am. Chem. Soc.* **2014**, *136*, 16335−16344.
(34) Kang, S.; Mo, Y.; Ong, S. P.; Ceder, G. A Facile Mechanism for Recharging Li_2O_2 in Li-O_2 Batteries. *Chem. Mater.* **2013**, *25*, 3328−3336.
(35) Zhang, Z.; Zhang, Q.; Chen, Y.; Bao, J.; Zhou, X.; Xie, Z.; Wei, J.; Zhou, Z. The First Introduction of Graphene to Rechargeable Li-CO_2 Batteries. *Angew. Chem., Int. Ed.* **2015**, *54*, 6550.
(36) Li, F.; Tang, D. M.; Chen, Y.; Golberg, D.; Kitaura, H.; Zhang, T.; Yamada, A.; Zhou, H. S. Ru/ITO: A Carbon-Free Cathode for Nonaqueous Li-O_2 Battery. *Nano Lett.* **2013**, *13*, 4702−4707.
(37) Xia, C.; Waletzko, M.; Chen, L. M.; Peppler, K.; Klar, P. J.; Janek, J. Evolution of Li_2O_2 Growth and Its Effect on Kinetics of Li-O_2. Batteries. *ACS Appl. Mater. Interfaces* **2014**, *6*, 12083−12092.
(38) Nasybulin, E. N.; Xu, W.; Mehdi, B. L.; Thomsen, E.; Engelhard, M. H.; Masse, R. C.; Bhattacharya, P.; Gu, M.; Bennett, W.; Nie, Z. M.; Wang, C. M.; Browning, N. D.; Zhang, J. G. Formation of Interfacial Layer and Long-Term Cyclability of Li-O_2 Batteries. *ACS Appl. Mater. Interfaces* **2014**, *6*, 14141−14151.
(39) Xiao, D. D.; Dong, S. M.; Guan, J.; Gu, L.; Li, S. M.; Zhao, N. J.; Shang, C. Q.; Yang, Z. H.; Zheng, H.; Chen, C.; Xiao, R. J.; Hu, Y. S.; Li, H.; Cui G. L.; Chen, L. Q. Direct Observation of Ordered Oxygen Defects on the Atomic Scale in Li_2O_2 for Li-O_2 Batteries. *Adv. Energy Mater.* **2015**, *5*, DOI: 10.1002/aenm.201400664.

DOI: 10.1021/acsami.5b08462
ACS Appl. Mater. Interfaces 2015, 7, 23798−23804